Pseudospin symmetry in single-particle resonances in spherical square wells

Bing-Nan Lu (吕炳楠),[1] En-Guang Zhao (赵恩广),[1,2] and Shan-Gui Zhou (周善贵)[1,2,*]

[1]*State Key Laboratory of Theoretical Physics, Institute of Theoretical Physics, Chinese Academy of Sciences, Beijing 100190, China*
[2]*Center of Theoretical Nuclear Physics, National Laboratory of Heavy Ion Accelerator, Lanzhou 730000, China*

Background: The pseudospin symmetry (PSS) has been studied extensively for bound states. Recently, we justified rigorously that the PSS in single-particle resonant states is exactly conserved when the attractive scalar and repulsive vector potentials of the Dirac Hamiltonian have the same magnitude but opposite sign [Phys. Rev. Lett. **109**, 072501 (2012)].

Purpose: To understand more deeply the PSS in single-particle resonant states, we focus on several issues related to the exact conservation and breaking mechanism of the PSS in single-particle resonances. In particular, we are interested in how the energy and width splittings of PS partners depend on the depth of the scalar and vector potentials.

Methods: We investigate the asymptotic behaviors of radial Dirac wave functions. Spherical square-well potentials are employed in which the PSS breaking part in the Jost function can be well isolated. By examining the zeros of Jost functions corresponding to small components of the radial Dirac wave functions, general properties of the PSS are analyzed.

Results: By examining the Jost function, the occurrence of intruder orbitals is explained and it is possible to trace continuously the PS partners from the PSS limit to the case with a finite potential depth. The dependence of the PSS in resonances as well as in bound states on the potential depth is investigated systematically. We find a threshold effect in the energy splitting and an anomaly in the width splitting of pseudospin partners when the depth of the single-particle potential varies from zero to a finite value.

Conclusions: The conservation and the breaking of the PSS in resonant states and bound states share some similar properties. The appearance of intruder states can be explained by examining the zeros of Jost functions. Origins of the threshold effect in the energy splitting and the anomaly in the width splitting of PS partners, together with many other problems, are still open and should be further investigated.

I. INTRODUCTION

More than 40 years ago, the pseudospin symmetry (PSS) was found to be approximately conserved in atomic nuclei and it was shown that doublets of single-particle levels with quantum numbers $(n_r, l, j = l + 1/2)$ and $(n_r - 1, l + 2, j = l + 3/2)$ in the same major shell are nearly degenerate [1,2]. Based on the pseudospin concept, a simple but useful pseudo-SU(3) model was proposed and later this model was generalized to be the pseudosymplectic model [3,4]. Since the PSS was observed, several nuclear phenomena have been interpreted in connection with the PSS, such as nuclear superdeformed configurations [5,6], identical bands [7,8], and pseudospin partner bands [9,10]. The PSS may also manifest itself in magnetic moments and transitions [11,12] and γ-vibrational states in atomic nuclei [13]. It is, thus, an interesting topic to investigate the origin and breaking mechanism of the PSS, which has been done within various backgrounds. With these studies a much better understanding of the nuclear structure based on the PSS is anticipated.

In early years much effort was devoted to revealing connections between the normal spin-orbit representation and the "pseudo" spin-orbit one and to exploring the microscopic origin of the PSS with spherical, axially deformed, and triaxially deformed potentials of (mostly) the oscillator type

[6,14–16]. It was found that the PSS conserves almost exactly for an oscillator potential with one-body orbit-orbit (v_{ll}) and spin-orbit (v_{ls}) interaction strengths satisfying the condition $v_{ls} \approx 4v_{ll}$; moreover, this condition is consistent with relativistic mean-field results [6]. A big step towards the understanding of the origin of the PSS in atomic nuclei was made in 1997 when Ginocchio revealed that the PSS is essentially a relativistic symmetry of the Dirac Hamiltonian and the pseudo-orbital angular momentum $\tilde{l}$ is nothing but the angular momentum of the small component of a Dirac spinor [17]. It was shown that the PSS in nuclei is exactly conserved when the scalar potential $S(r)$ and the vector potential $V(r)$ have the same size but opposite sign, i.e., $\Sigma(r) \equiv S(r) + V(r) = 0$ [17]. Later Meng *et al.* found that the PSS is connected with the competition between the centrifugal barrier and the pseudospin-orbit potential and the PSS is exact under the condition $d\Sigma(r)/dr = 0$ [18]. This condition means that the PSS becomes much better for exotic nuclei with a highly diffused potential [19]. However, in either limit, $\Sigma(r) = 0$ or $d\Sigma(r)/dr = 0$, there are no longer bound states; thus, in realistic nuclei, the PSS is always broken. In this sense, the PSS is usually viewed as a dynamical symmetry [20,21]. Following discussions for spherical nuclei, the study of the PSS within the relativistic framework was quickly extended to deformed ones [22,23]. One consequence of the fact that the PSS is a relativistic symmetry of the Dirac Hamiltonian is that the relativistic wave functions of the corresponding pseudospin

doublets satisfy certain relations which have been tested both in spherical and in deformed nuclei [22,24–26].

By solving the Dirac Hamiltonian, one gets not only positive energy states in the Fermi sea but also negative energy states in the Dirac sea. When solutions of the Dirac Hamiltonian are used as a complete basis, e.g., in the Dirac Woods-Saxon basis, states with both positive and negative energies must be included [27–31]. Negative energy states correspond to antiparticle states. In both seas, there are discrete bound states and continuum states. The PSS study has been generalized not only from the Fermi sea to the Dirac sea, i.e., from single-particle states to antiparticle states, but also from bound states to continuum states. The PSS in negative energy states means the spin symmetry (SS) in antinucleon spectra [32,33]. The SS in single antinucleon spectra was explored and found to be much better developed than the PSS in normal nuclear single-particle spectra [33]. The SS in antinucleon spectra was also tested by investigating relations between Dirac wave functions of spin doublets with the relativistic mean-field model [34]. Later the SS in antiparticle spectrum was studied with the relativistic Hartree-Fock model and the contribution from the Fock term was discussed [35]. It has been pointed out in Ref. [33] that one open problem related to the study of the SS in antinucleon spectra is the polarization effect caused by the annihilation of an antinucleon in a normal nucleus. Detailed calculations of the antibaryon ($\bar{p}$, $\bar{\Lambda}$, etc.) annihilation rates in the nuclear environment showed that the in-medium annihilation rates are strongly suppressed by a significant reduction of the reaction Q values, leading to relatively long-lived antibaryon-nucleus systems [36]. Recently the SS in the anti-Λ spectrum of hypernuclei was studied quantitatively [37]; this kind of study would be of great interests for possible experimental tests.

The SS and PSS have been investigated extensively within the relativistic framework. The readers are referred to Ref. [38] for a review and to Ref. [39] for an overview of recent progresses. Next we briefly mention several aspects of these progresses. The node structure of radial Dirac wave functions of pseudospin doublets was studied in Ref. [40], which was helpful particularly for the understanding of the special status of nodeless intruder states in nuclei. Although there are some doubts about the connection between the PSS and conditions $\Sigma(r) = 0$ or $d\Sigma(r)/dr = 0$ [41], following the idea that under these conditions the PSS is conserved exactly, a lot of discussions have been made about the PSS and/or SS in single-(anti-)particle spectra obtained by exactly or approximately solving the Dirac Hamiltonian with various potentials [42–53]. One of interesting topics is the tensor effect on the PSS or SS which have been investigated in some of the above-mentioned work and some others, e.g., in Refs. [54–57]. Much effort was also devoted to the study of the perturbative feature of the breaking of the PSS [39,58,59]. The concept of supersymmetry (SUSY) and the similarity renormalization group method were both used in the study of the PSS and/or SS by several groups [39,60,61]. The relevance of the PSS in the structure of halo nuclei [56] and superheavy nuclei [62,63] was also found. Quite recently, the node structure of radial Dirac wave functions in central confining potentials was studied and the authors have shown in a general way that it is possible to have

positive energy bound solutions for these potentials under the condition of exact PSS [64]. Note that there have been some investigations of PSS connected with some specific forms of confining potentials [65]. Finally, we mention that there have been some discussions on the physics behind $\Sigma(r) \approx 0$ or $d\Sigma(r)/dr \approx 0$ [66,67] and more investigations are expected.

In recent years, there has been an increasing interest in the exploration of continuum and resonant states, especially in the study of exotic nuclei with unusual N/Z ratios. In these nuclei, the neutron (or proton) Fermi surface is close to the particle continuum; thus, the contribution of the continuum is important [28,68–75]. Many methods or models developed for the study of resonances [76] have been adopted to locate the position and to calculate the width of a nuclear resonant state, e.g., the analytical continuation in coupling constant (ACCC) method [77,78], the real stabilization method (RSM) [79–81], the complex scaling method (CSM) [82], the coupled-channels method [83,84], and some others [85,86]. Each of these methods has advantages and disadvantages. For example, the RSM is very powerful for narrow resonances and the CSM for broad ones.

The study of symmetries in resonant states is certainly interesting; one of the topics is the PSS in the continuum. We note that the PSS and/or SS in nucleon-nucleus and nucleon-nucleon scatterings have been investigated [87,88]. Meanwhile, there were also some numerical investigations of the PSS in single-particle resonances [89,90] and the SS in single-particle resonant states [91]. Recently, we gave a rigorous justification of the PSS in single-particle resonant states [92]. We have shown that the PSS in single-particle resonant states in nuclei is exactly conserved under the same condition for the PSS in bound states. i.e., $\Sigma(r) = 0$ or $d\Sigma(r)/dr = 0$ [92,93]. As we noted in Ref. [92], it is straightforward to extend the study of the PSS in resonant states in the Fermi sea to that in the negative energy states in the Dirac sea or SS in antiparticle continuum spectra. In the present work we will focus on several open problems related to the exact conservation and breaking mechanism of the PSS in single-particle resonances. To this end spherical square-well potentials are employed in which the PSS breaking part can be separated from other parts in the Jost function. By examining zeros of Jost functions corresponding to small components of radial Dirac wave functions, we examine general properties of PSS splittings of the energies and widths.

In Sec. II, the justification of the PSS in single-particle resonant states will be given briefly and the emphasis will be put on the mechanism of the exact conservation and breaking of pseudospin symmetry in single-particle resonant states in square-well potentials. Details on the study of the PSS in single-particle resonances will be presented in Sec. III. In Sec. IV, we will summarize this work and mention some perspectives.

II. PSEUDOSPIN SYMMETRY IN SINGLE-PARTICLE RESONANT STATES IN SQUARE-WELL POTENTIALS

A rigorous justification of the PSS in single-particle resonant states has been given in Ref. [92]. For completeness,

we will briefly mention it before we discuss the PSS in square-well potentials.

In relativistic mean-field models, the covariant functional can be one of the following four forms: the meson exchange or point-coupling nucleon interactions combined with the nonlinear or density-dependent couplings [69,70,94–98]. The starting point of the covariant density functional with the nonlinear point couplings is the following Lagrangian:

$$\mathcal{L} = \bar{\psi}(i\gamma_\mu \partial^\mu - M)\psi - \mathcal{L}_{\text{lin}} - \mathcal{L}_{\text{nl}} - \mathcal{L}_{\text{der}} - \mathcal{L}_{\text{Cou}}, \quad (1)$$

where

$$
\begin{aligned}
\mathcal{L}_{\text{lin}} &= \frac{1}{2}\alpha_S \rho_S^2 + \frac{1}{2}\alpha_V (j_V)_\mu j_V^\mu \\
&\quad + \frac{1}{2}\alpha_{TS}(\vec{\rho}_{TS})^2 + \frac{1}{2}\alpha_{TV}(\vec{j}_{TV})_\mu \cdot \vec{j}_{TV}^\mu, \\
\mathcal{L}_{\text{nl}} &= \frac{1}{3}\beta_S \rho_S^3 + \frac{1}{4}\gamma_S \rho_S^4 + \frac{1}{4}\gamma_V [(j_V)_\mu j_V^\mu]^2, \\
\mathcal{L}_{\text{der}} &= \frac{1}{2}\delta_S \partial_\nu \rho_S \partial^\nu \rho_S + \frac{1}{2}\delta_V \partial_\nu (j_V)_\mu \partial^\nu j_V^\mu \\
&\quad + \frac{1}{2}\delta_{TS} \partial_\nu \vec{\rho}_{TS} \cdot \partial^\nu \vec{\rho}_{TS} + \frac{1}{2}\delta_{TV} \partial_\nu (\vec{j}_{TV})_\mu \cdot \partial^\nu \vec{j}_{TV}^\mu, \\
\mathcal{L}_{\text{Cou}} &= \frac{1}{4}F^{\mu\nu}F_{\mu\nu} + e\frac{1-\tau_3}{2}A_\mu j_V^\mu,
\end{aligned}
\quad (2)
$$

are the linear coupling, nonlinear coupling, derivative coupling, and the Coulomb part, respectively. M is the nucleon mass, α_S, α_V, α_{TS}, α_{TV}, β_S, γ_S, γ_V, δ_S, δ_V, δ_{TS}, and δ_{TV} are coupling constants for different channels and e is the electric charge. ρ_S, $\vec{\rho}_{TS}$, j_V, and $\vec{j}_{TV}$ are the isoscalar density, isovector density, isoscalar current, and isovector current, respectively. The various densities and currents are defined as

$$\rho_S = \bar{\psi}\psi, \quad \vec{\rho}_{TS} = \bar{\psi}\vec{\tau}\psi, \quad (3)$$

$$j_V^\mu = \bar{\psi}\gamma^\mu\psi, \quad \vec{j}_{TV}^\mu = \bar{\psi}\vec{\tau}\gamma^\mu\psi. \quad (4)$$

The equation of motion for nucleons, the Dirac equation, is derived from the Lagrangian density as

$$\{\boldsymbol{\alpha} \cdot \boldsymbol{p} + \beta[M + S(\boldsymbol{r})] + V(\boldsymbol{r})\}\psi(\boldsymbol{r}) = \epsilon\psi(\boldsymbol{r}), \quad (5)$$

where $\boldsymbol{\alpha}$ and β are Dirac matrices and M is the nucleon mass. In Eq. (5), the scalar potential $S(\boldsymbol{r})$ and the vector potential $V(\boldsymbol{r})$ are determined by densities and currents defined in Eqs. (3) and (4). It turns out that both potentials are very deep, but they have opposite signs: The scalar potential $S(\boldsymbol{r})$ is attractive and the vector potential $V(\boldsymbol{r})$ is repulsive. This results in an approximate PSS in nuclear single-particle spectra [17] and an even better conserved SS in antinucleon spectra [33].

For a spherical nucleus, the Dirac spinor reads

$$\psi(\boldsymbol{r}) = \frac{1}{r}\begin{pmatrix} i F_{n\kappa}(r)Y_{jm}^l(\theta,\phi) \\ -G_{\tilde{n}\kappa}(r)Y_{jm}^{\tilde{l}}(\theta,\phi) \end{pmatrix}, \quad (6)$$

where $Y_{jm}^l(\theta,\phi)$ is the spin spherical harmonic and $F_{n\kappa}(r)/r$ and $G_{\tilde{n}\kappa}(r)/r$ are the radial wave functions for the upper and lower components with n and $\tilde{n}$ numbers of radial nodes. The total angular momentum j, the orbit angular momentum l, and the pseudo-orbital angular momentum $\tilde{l}$ are determined by κ

through

$$
\begin{aligned}
j &= |\kappa| - \frac{1}{2}, \\
l(l+1) &= \kappa(\kappa+1), \quad l \geqslant 0, \\
\tilde{l}(\tilde{l}+1) &= \kappa(\kappa-1), \quad \tilde{l} \geqslant 0.
\end{aligned}
\quad (7)
$$

The radial Dirac equation reads

$$\begin{pmatrix} M + \Sigma(r) & -\frac{d}{dr} + \frac{\kappa}{r} \\ \frac{d}{dr} + \frac{\kappa}{r} & -M + \Delta(r) \end{pmatrix}\begin{pmatrix} F(r) \\ G(r) \end{pmatrix} = \epsilon\begin{pmatrix} F(r) \\ G(r) \end{pmatrix}, \quad (8)$$

where $\Sigma(r) = V(r) + S(r)$, $\Delta(r) = V(r) - S(r)$, and ϵ is the eigenenergy. For brevity we omit the subscripts from $F(r)$ and $G(r)$. This first-order coupled equation can be rewritten as two decoupled second-order differential ones by eliminating either the large or the small component [18,19,33],

$$
\begin{aligned}
&\left[\frac{d^2}{dr^2} + \frac{1}{M_+(r)}\frac{d\Delta(r)}{dr}\frac{d}{dr} - \frac{l(l+1)}{r^2}\right. \\
&\quad \left. + \frac{1}{M_+(r)}\frac{\kappa}{r}\frac{d\Delta(r)}{dr} - M_+(r)M_-(r)\right]F(r) = 0, \quad (9) \\
&\left[\frac{d^2}{dr^2} - \frac{1}{M_-(r)}\frac{d\Sigma(r)}{dr}\frac{d}{dr} - \frac{\tilde{l}(\tilde{l}+1)}{r^2}\right. \\
&\quad \left. + \frac{1}{M_-(r)}\frac{\kappa}{r}\frac{d\Sigma(r)}{dr} - M_+(r)M_-(r)\right]G(r) = 0, \quad (10)
\end{aligned}
$$

where $M_+(r) = M + \epsilon - \Delta(r)$ and $M_-(r) = M - \epsilon + \Sigma(r)$. In Ref. [99], it has been shown that each of these two Schrödinger-like equations, together with its charge-conjugated one, are fully equivalent to Eq. (5). Note that for bound states, there is always a singularity in $1/M_-(r)$ in Eq. (10). For resonant states we discuss here, such a singularity does not exist.

For the continuum in the Fermi sea, i.e., $\epsilon \geqslant M$, there exist two independent solutions for Eqs. (9) or (10). The physically acceptable one is the solution that vanishes at the origin. For example, the regular solution for the small component $G(r)$ behaves like $j_{\tilde{l}}(pr)$ as $r \to 0$,

$$\lim_{r\to 0} G(r)/j_{\tilde{l}}(pr) = 1, \quad p = \sqrt{\epsilon^2 - M^2}. \quad (11)$$

Since the PSS is directly connected with the small component, we will mainly focus on Eq. (10) in the following discussions. At large r potentials for neutrons vanish, the regular solution is written as a combination of Riccati-Hankel functions,

$$G(r) = \frac{i}{2}\left[\mathcal{J}_\kappa^G(p)h_{\tilde{l}}^-(pr) - \mathcal{J}_\kappa^G(p)^* h_{\tilde{l}}^+(pr)\right], \quad r \to \infty, \quad (12)$$

where $h_{\tilde{l}}^\pm(pr)$ are the Ricatti-Hankel functions. $\mathcal{J}_\kappa(p)$ is the Jost function which is an analytic function of p and can be analytically continued to a large region in the complex p plane. The zeros of $\mathcal{J}_\kappa^G(p)$ on the positive imaginary axis of the p plane correspond to bound states and those on the lower p plane and near the real axis correspond to resonant states. The resonance energy E and width Γ are determined by the relation $E - i\Gamma/2 = \epsilon - M$.

In the PSS limit, Eq. (10) is reduced as

$$\left[\frac{d^2}{dr^2} - \frac{\tilde{l}(\tilde{l}+1)}{r^2} + (\epsilon - M)M_+(r)\right]G(r) = 0. \quad (13)$$

For pseudospin doublets with κ and $\kappa' = -\kappa + 1$, the small components satisfy the same equation because they have the same pseudo-orbital angular momentum $\tilde{l}$. For continuum states, $G_\kappa(\epsilon, r) = G_{\kappa'}(\epsilon, r)$ is true for any energy ϵ; thus, we have $\mathcal{J}_{\kappa'}^G(p) = \mathcal{J}_\kappa^G(p)$. This equivalence can be generalized into the complex p plane due to the uniqueness of the analytic continuation. Thus, the zeros are the same for $\mathcal{J}_{\kappa'}^G(p)$ and $\mathcal{J}_\kappa^G(p)$ and the PSS in single-particle resonant states in nuclei is exactly conserved. Note that when we focus on the zeros of Jost functions of pseudospin doublets on the positive imaginary axis of the p plane, we come to the well-known PSS for bound states. For bound states this is an alternative way to justify the PSS or SS besides those ways in which the Dirac equation and Dirac wave functions are examined in, e.g., Refs. [17,18,22,33] or introducing the concept of SUSY and the similarity renormalization group method [39,60,61]. For single-particle resonant states, to now this is the only way to do so.

In Fig. 1 we show spherical potentials $\Sigma(r)$ and $\Delta(r)$ of ^{208}Pb calculated using the relativistic mean-field model with the parameter set PC-PK1 [100]. However, to extract the energy and width of resonant states in such potentials is relatively complex. In particular, when we want to study the PSS and examine the origin and the splitting mechanism, it is better to start from solvable models. In Fig. 1 we show two types of potentials which can be used to approximate the realistic one, the Woods-Saxon and square-well potentials. For ^{208}Pb the radius is around 7 fm and the depths of potentials are 650 and 66 MeV, respectively; these parameters of Woods-Saxon potentials have been proposed in Ref. [89]. Although the diffuseness of realistic potentials cannot be included, it is still a good starting point to study general properties of the PSS for the resonant as well as bound states by using square-well potentials because the PSS-breaking term in the Jost function is separated from the PSS-conserving term.

Spherical square-well potentials for $\Sigma(r)$ and $\Delta(r)$ read

$$\Sigma(r) = \begin{cases} C, & r < R, \\ 0, & r \geqslant R, \end{cases} \quad (14)$$

$$\Delta(r) = \begin{cases} D, & r < R, \\ 0, & r \geqslant R, \end{cases} \quad (15)$$

where C and D are depths and R is the width. The Jost function $\mathcal{J}_\kappa^G(p)$ is derived as [92]

$$\mathcal{J}_\kappa^G(p) = -\frac{p^{\tilde{l}}}{2ik^{\tilde{l}+1}}\left\{ j_{\tilde{l}}(kR)ph_{\tilde{l}}^{+\prime}(pR) - kj_{\tilde{l}}'(kR)h_{\tilde{l}}^+(pR) \right.$$
$$\left. - \frac{C}{\epsilon - M - C}\left[kj_{\tilde{l}}'(kR) - \frac{\kappa}{R}j_{\tilde{l}}(kR)\right]h_{\tilde{l}}^+(pR) \right\}, \quad (16)$$

with $k = \sqrt{(\epsilon - C - M)(\epsilon - D + M)}$. The PSS in both bound states and resonant states can be explained explicitly. If $C = 0$, the second term in $\mathcal{J}_\kappa^G(p)$ vanishes and the first term only depends on the pseudo-orbital angular momentum $\tilde{l}$. Then
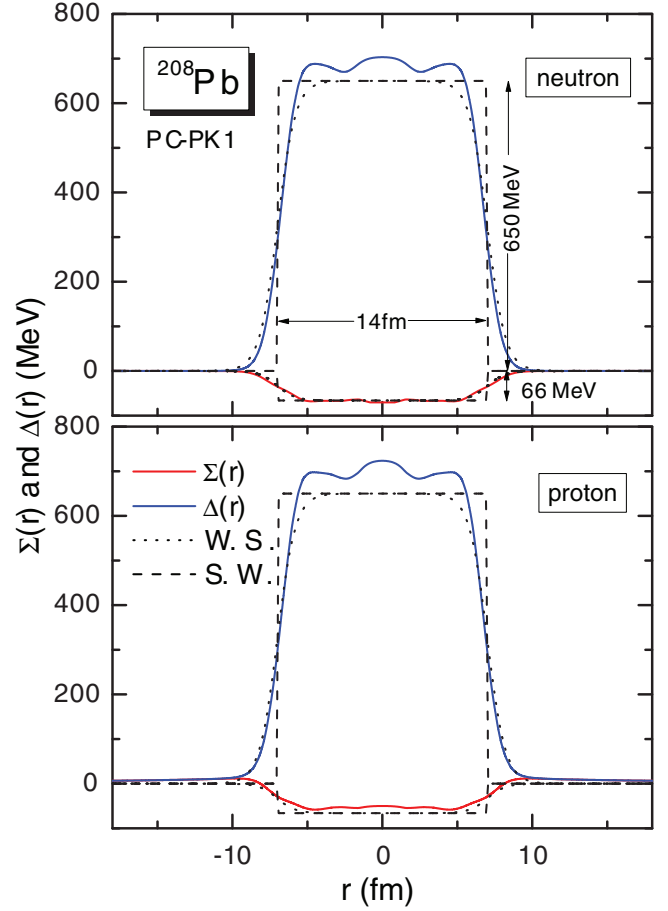

FIG. 1. (Color online) Potentials $\Sigma(r)$ and $\Delta(r)$ of ^{208}Pb calculated using the relativistic mean-field model with the parameter set PC-PK1 [100]. These potentials can be approximated by Woods-Saxon (W.S.) potentials (dotted curves) or spherical square-well (S.W.) potentials (dashed lines) with a radius around 7 fm and depths around 650 and 66 MeV. The long tails in the proton case are due to the Coulomb interaction.

Jost functions with different κ but the same $\tilde{l}$ are identical, and energies and widths of resonant pseudospin partners are exactly the same.

For the large component $F(r)$ we can write a similar expression for the asymptotic behavior,

$$F(r) = \frac{i}{2}\left[\mathcal{J}_\kappa^F(p)h_l^-(pr) - \mathcal{J}_\kappa^F(p)^* h_l^+(pr)\right], \quad r \to \infty. \quad (17)$$

At the origin,

$$\lim_{r\to 0} F(r)/j_l(pr) = 1, \quad p = \sqrt{\epsilon^2 - M^2}. \quad (18)$$

In square-well potentials, $\mathcal{J}_\kappa^F(p)$ is derived as

$$\mathcal{J}_\kappa^F(p) = -\frac{p^l}{2ik^{l+1}}\left\{ j_l(kR)ph_l^{+\prime}(pR) - kj_l'(kR)h_l^+(pR) \right.$$
$$\left. - \frac{D}{\epsilon + M - D}\left[kj_l'(kR) + \frac{\kappa}{R}j_l(kR)\right]h_l^+(pR) \right\}. \quad (19)$$
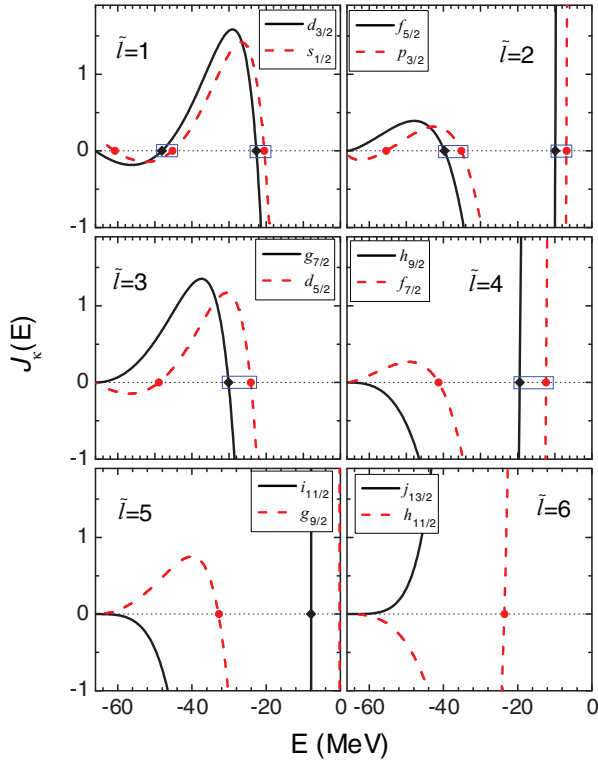
FIG. 2. (Color online) The Jost function $\mathcal{J}_\kappa(E)$ (in arbitrary unit) on the real E axis for several pairs of pseudospin partners. The results for pseudospin $\tilde{s} = \pm 1/2$ are denoted as solid and dashed curves, respectively. The zero points representing bound states with $\tilde{s} = \pm 1/2$ are denoted as black and red dots, respectively.

It looks similar to that of the small component $\mathcal{J}_\kappa^G(p)$, with the exception that the potential parameter C is substituted by D and the pseudo-orbital angular momentum $\tilde{l}$ is substituted by l. In the case of $D \to 0$, this form of Jost function can be used to investigate the spin symmetry of single-particle levels.

By examining the zeros of the Jost function, we will study properties of single-particle bound states and resonant states and the PSS.

III. RESULTS AND DISCUSSIONS

A. The Jost function and its zeros and the occurrence of intruder states

Now we examine the Jost function (16) corresponding to the small component of the radial Dirac wave function in square-well potentials with $C = -66$ MeV and $D = 650$ MeV. For bound states, one can draw the Jost function as a function of either the imaginary part of p or the binding energy $E \equiv \epsilon - M$. Here we use the latter in order to have a more intuitive picture for the energy splitting. Such Jost functions $\mathcal{J}_\kappa(E)$ for several pairs of pseudospin partners are shown in Fig. 2. In the following discussions, we omit the superscript "G" from $\mathcal{J}_\kappa(E)$. The results for pseudospin $\tilde{s} = \pm 1/2$ are denoted as solid and dashed curves, respectively. The zero points representing bound states with $\tilde{s} = \pm 1/2$ are denoted as black and red dots, respectively. For each pseudo-orbital angular momentum $\tilde{l}$ there exist two κ's, one with a positive value $\kappa = \tilde{l} + 1$ and the other with a negative value $\kappa = -\tilde{l}$, respectively. For example, for $\tilde{l} = 1$ ($\tilde{p}$) we have $\kappa = 2$ (pseudospin aligned, $d_{3/2}$) or $\kappa = -1$ (pseudospin antialigned, $s_{1/2}$). There are some common features in these Jost functions which will be detailed in the following.

First, the number of zeros for Jost functions with negative κ is always one more than that with positive κ if the nonphysical node at the bottom of the potential is excluded. For example, for $\tilde{l} = 1$ there are two zeros for $d_{3/2}$ ($\kappa = 2$) but three for $s_{1/2}$ ($\kappa = -1$); this means that there are two bound states for $d_{3/2}$ and three for $s_{1/2}$. Therefore, there is always one bound state with $\kappa < 0$ which does not have a partner; this state is simply an intruder state. The study of the node structure of radial Dirac wave functions of pseudospin doublets has been made in which the occurrence of nodeless intruder states has been explained [40]. This kind of study was also extended to the Dirac sea [33] and to the case with confining potentials [64,65]. Note that for harmonic oscillator (HO) potentials or some combination of HO and Woods-Saxon potentials, bound states exist even under the condition of the exact PSS and intruder states do have pseudospin partners [65]. The reason why there are intruder states was also naturally explained by employing both exact and broken SUSY within a unified scheme [39,60,101]. Here we present a novel way to show the origin of the appearance of intruder states: The lowest zero of the Jost function (16) with negative κ is always isolated while the others are paired off with those of the Jost function with positive κ.

Second, the similarity of Jost functions can also be used as a test of the PSS or SS symmetries besides the examination of radial wave functions of PSS or SS doublets [22,24–26, 34,57,90]. From Fig. 2, one finds that except in the energy range around and below the first zero of the Jost function with negative κ, Jost functions corresponding to PSS doublets, i.e., with the same $\tilde{l}$, are similar with each other. This is particularly clear for the cases with small $\tilde{l}$, e.g., $\tilde{l} = 1$. Furthermore, in the low-energy range above the first zero of the Jost function with negative κ, these Jost functions are rather smooth. When approaching the threshold, the Jost function becomes very steep against the energy. Although the absolute differences between $\mathcal{J}_\kappa$'s are large, the zeros corresponding to PS doublets are still not far from each other, which means a good PSS.

Third, the difference between Jost functions with the same $\tilde{l}$ increases when $\tilde{l}$ becomes larger, as is the difference of the positions of their paired zeros. That is, the splitting between the energy (in short, the energy splitting) of pseudospin partners increases with $\tilde{l}$, which is consistent with earlier studies, e.g., in Ref. [19,22]. This can be explained by the factor κ of the pseudospin splitting term $\kappa j_{\tilde{l}}(kR)/R$ in Eq. (16) which breaks the PSS and will be discussed in the next subsection in details.

B. Single-particle spectra and pseudospin splittings in the energy and the width

There is no analytical solution for $\mathcal{J}_\kappa(p) = 0$. However, because the Jost function is analytic near its zeros, one can easily get the roots of $\mathcal{J}_\kappa(p) = 0$ by using the secant method.
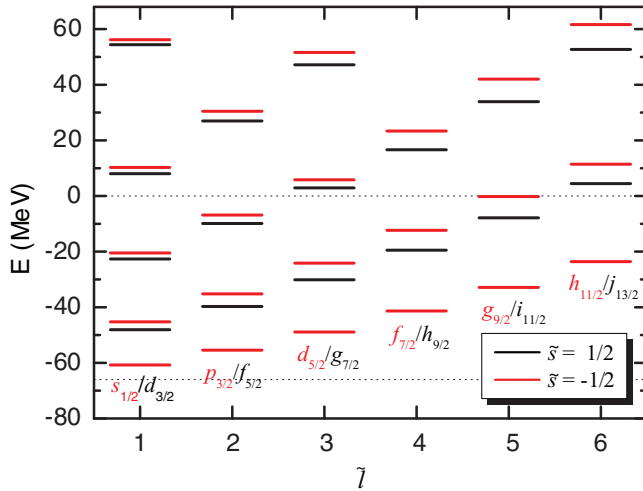
FIG. 3. (Color online) Energies of bound states as well as resonances with $\tilde{l} = 1, 2, \ldots, 6$ in spherical square-well potentials with $C = -66$ MeV and $D = 650$ MeV. The results with pseudospin $\tilde{s} = \pm 1/2$ are denoted as black and red lines, respectively. The bottom of the potential well $E = -66$ MeV and the threshold $E = 0$ are shown as dotted lines. For each pseudo-orbital angular momentum $\tilde{l}$ the lowest level is an intruder state and has no pseudospin partner.

Starting from an initial guess for a root, the iteration usually converges after a few steps [92].

In Fig. 3 we show the energies of the bound states as well as the resonances with $\tilde{l} = 1, 2, \ldots, 6$ in square-well potentials with $C = -66$ MeV and $D = 650$ MeV. The results with pseudospin $\tilde{s} = \pm 1/2$ are denoted as black and red lines, respectively. To see PSS splittings more clearly, the results are depicted with respect to the pseudo-orbital angular momentum $\tilde{l}$. For example, for $\tilde{l} = 3$ we have put together levels with $g_{7/2}$ ($\tilde{s} = 1/2$ and $\kappa = 4$) and those with $d_{5/2}$ ($\tilde{s} = -1/2$ and $\kappa = -3$).

As explained in the previous subsection, for each pseudo-orbital angular momentum $\tilde{l}$, the lowest level represents an intruder state which has no pseudospin partner. In Fig. 3, one finds the normal energy splitting, i.e., for a pair of pseudospin doublet states, the one with $\tilde{s} = -1/2$ is higher in energy than that with $\tilde{s} = 1/2$, regardless if these states are bound or in the continuum. For bound states, this is well known, though in some realistic calculations, e.g., Refs. [19,22,102], it is shown that there are some exceptions. For resonant states, from Refs. [89,90], one finds that, in many cases, for a pair of pseudospin doublet states, the one with $\tilde{s} = -1/2$ is lower in energy. Systematic studies have been carried out to investigate the parameter (the depth, the radius, and the diffuseness) dependence of the PSS in resonances in Woods-Saxon potentials and the isospin dependence of the PSS in resonances in RMF potentials [89]. It was found that in these more realistic potentials, the energy splitting of pseudospin doublets in continuum has a complicated dependence on the parameters of the potential and on the ratio of neutron and proton numbers [89].

For bound states, when approaching the threshold, the energy splitting becomes smaller for all $\tilde{l}$ as shown in Fig. 3. This means that the PSS becomes more conserved for orbitals
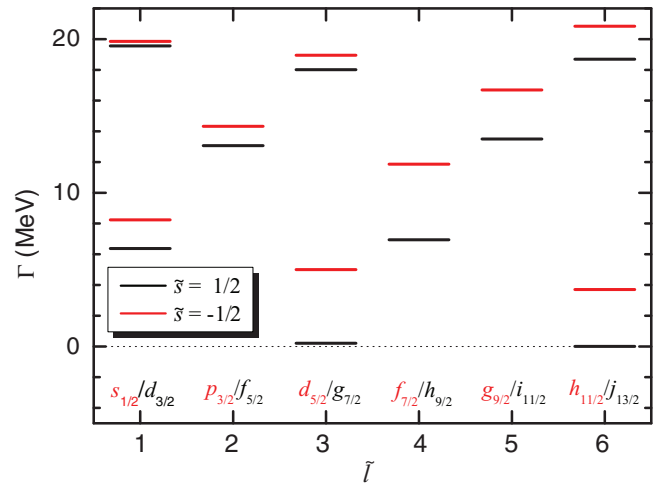

FIG. 4. (Color online) Widths of resonant states with $\tilde{l} = 1, 2, \ldots, 6$ in spherical square-well potentials with $C = -66$ MeV and $D = 650$ MeV. The results with pseudospin $\tilde{s} = \pm 1/2$ are denoted as black and red lines, respectively. The bound-state threshold $E = 0$ is shown as a dotted line.

which are closer to the continuum, which has been found and explained [17–19,22]. In the present work, we can explain this point by examining the Jost function (16). The pseudospin splitting term in Eq. (16) is proportional to $C/(\epsilon - M - C)$ and the denominator $\epsilon - M - C$ means the relative energy with respect to the bottom of the single-particle potential. Apparently, for less bound states, the factor $C/\epsilon - M - C$ is smaller and the pseudospin splitting term in the Jost function are less important; consequently, the PSS becomes better.

As we noticed earlier, the pseudospin splitting term in Eq. (16) depends not only on the binding energy but also on $\tilde{l}$ and κ. Thus, the energy splitting becomes larger as the pseudo-orbital angular momentum $\tilde{l}$ increases. Especially if we focus on the levels with the same number of radial nodes, the energy splitting monotonically increases with $\tilde{l}$; this behavior has been observed for bound states in many publications [18,19,22,33].

For resonant states, not only the energies but also the widths are of importance. In Fig. 4 we show the calculated widths of resonances in spherical square-well potentials with $C = -66$ MeV and $D = 650$ MeV. Comparing this figure with Fig. 3, one finds that the width splitting shares several similar features with the energy splitting. First, the width of the resonant state with $\tilde{s} = -1/2$ is always larger than that of its pseudospin partner with $\tilde{s} = 1/2$. Note that the width splitting depends on the depth the potential C, as will be shown in Sec. III C. Second, the width splitting decreases when the energy of resonant states increases for the same $\tilde{l}$. For the resonances with very high energies, the width splitting even becomes negligible.

From Fig. 3, one finds that for resonant states, when the energy increases, the energy splitting becomes smaller for $\tilde{l} = 1$. But it becomes a bit larger for $\tilde{l} = 3$ and 5, which seems to contradict the fact that the factor of the pseudospin splitting term in Eq. (16), i.e., $C/(\epsilon - M - C)$, becomes smaller in amplitude when the ϵ becomes larger. However,
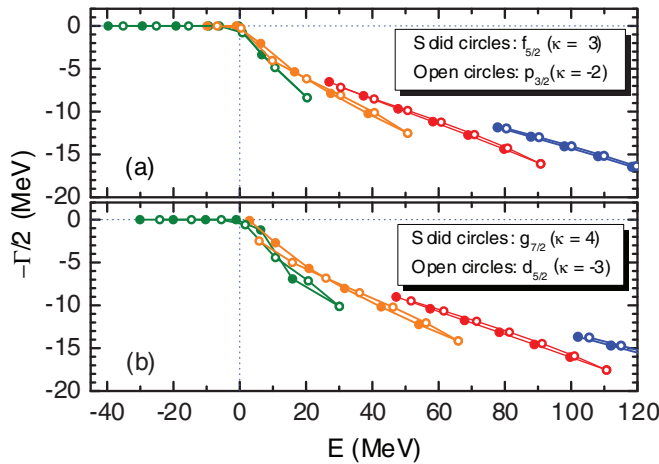
FIG. 5. (Color online) Zeros of the Jost function $\mathcal{J}_\kappa(E)$ in spherical square-well potentials with different potential depth $C = -70, -60, \ldots, 0$ MeV for (a) $\tilde{l} = 2$: $p_{3/2}$ ($\kappa = -2$) and $f_{5/2}$ ($\kappa = 3$); and (b) $\tilde{l} = 3$: $d_{5/2}$ ($\kappa = -3$) and $g_{7/2}$ ($\kappa = 4$). When $C = 0$, pseudospin doublets are degenerate and corresponding symbols overlap each other. The results with pseudospin $\tilde{s} = \pm 1/2$ are denoted as solid and open circles, respectively. When $C = -70$ MeV, energies of intruder states are below -40 MeV and not shown.

this is not really a contradiction because, for a resonant state, one should take into account both the energy and the width. For the closeness of pseudospin partners in the continuum, one should check the distance between them in the complex energy or momentum plane. As shown in Fig. 5, for $\tilde{l} = 2$ or 3, the distance between the n-th pair of pseudospin resonant doublets is always smaller than that between the $(n-1)$-th pair when the potential depth is fixed. Note that in Fig. 5 are presented bound states and resonant states in spherical square-well potentials with $C = -70, -60, \ldots, 0$ MeV.

Differing from the energy splitting which increases when $\tilde{l}$ increases, from Fig. 4 it is seen that when the radial quantum number is fixed, the width splitting decreases with $\tilde{l}$, which seems inconsistent with the dependence of the pseudospin splitting term in Eq. (16) on $\tilde{l}$ and κ. To solve this puzzle, one again needs to examine the distance between PS partners in the complex energy or momentum plane. In Fig. 5, one can find that, at fixed C and radial quantum number, e.g., comparing the red curves in Figs. 5(a) and 5(b), the pair of $\tilde{l} = 2$ pseudospin resonant partners is always closer than those of $\tilde{l} = 3$.

C. The dependence of the PSS in resonances on the depth of the potential: A threshold effect in the energy splitting and an anomaly in the width splitting

Since the potential depth is relevant mostly to the energy and width of a resonant state, next we study how the PSS evolves with the variation of the potential depth C. In Fig. 5 we show zeros of Jost functions $\mathcal{J}_\kappa(E)$ in the spherical square-well potentials with different potential depth $C = -70, -60, \ldots, 0$ MeV for $\tilde{l} = 2$ [$p_{3/2}$ ($\kappa = -2$) and $f_{5/2}$ ($\kappa = 3$)] and $\tilde{l} = 3$ [$d_{5/2}$ ($\kappa = -3$) and $g_{7/2}$ ($\kappa = 4$)]. Results with pseudospin $\tilde{s} = \pm 1/2$ are denoted as solid and open dots, respectively. For simplicity the results are shown in the com-
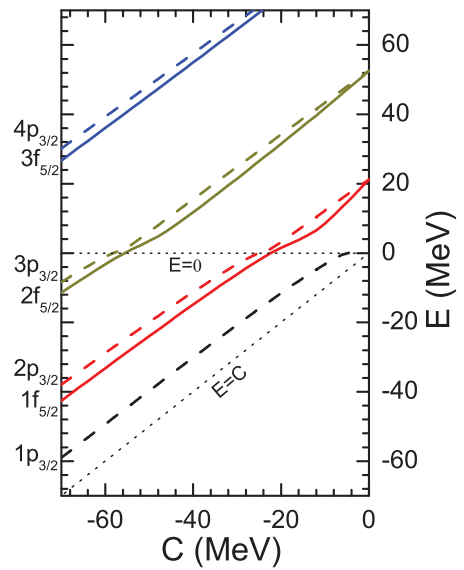

FIG. 6. (Color online) Energies of bound and resonant states for $p_{3/2}$ and $f_{5/2}$ with $\tilde{l} = 2$ in spherical-well potentials as functions of the potential depth C. The results with pseudospin $\tilde{s} = \pm 1/2$ are denoted as solid and dashed curves, respectively. All the levels are paired off except for the lowest one. The bottom of the potential $E = C$ and the bound state threshold $E = 0$ are shown as dotted lines.

plex energy plane. In the PSS limit, that is, $C = V + S = 0$, the zeros are paired off and each pair of states coincide with each other, which is consistent with the formal analysis. When the potential depth increases, the zeros move gradually to the up left corner, i.e., both the energy and the width become smaller. Meanwhile, the paired pseudospin partners separate from each other, which means the PSS is broken. However, the distance between the paired points is not big and the PSS is conserved approximately.

In Fig. 6 we show the calculated energies of bound and resonant states with $\tilde{l} = 2$ in the square-well potentials as functions of the potential depth C. As the potential depth varies from 0 to -70 MeV, the energies are always paired off except for the lowest one. In the PSS limit, i.e., $C = 0$, there is no bound state and all the levels are resonant states with finite widths. The PSS is exactly manifested in this case. When the single-particle potential becomes deeper, the energies of both pseudospin partners decrease and the energy splitting first increases and then decreases. After one of the pseudospin partners becomes a bound state, an interesting phenomenon appears, that is, one level is still a resonant state while the other level becomes bound. Due to the PSS, their energies are almost the same, except that one is a little bit higher than the threshold while another is a little bit lower. Because a resonant state is very close to the threshold, the corresponding width is also rather small. In other words, the pseudospin partner of a single-particle bound state may be another bound state or a "quasibound" state with very long lifetime. When the depth of the potential increases further, both of the pseudospin partners become bound states. In this case we can discuss the usual PSS for bound states.
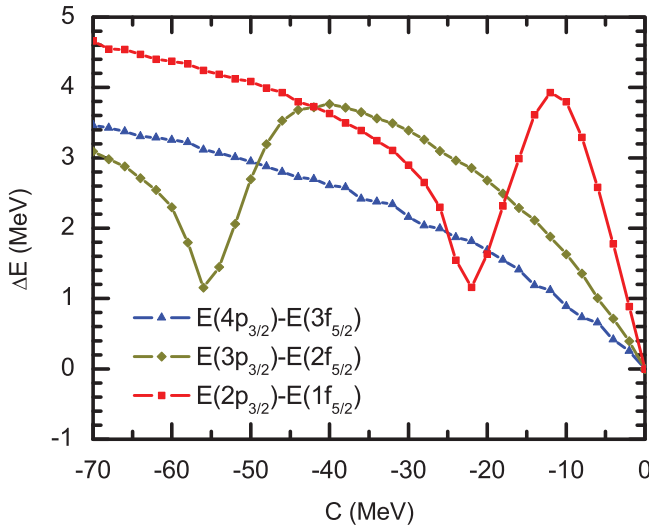
FIG. 7. (Color online) The energy splitting between PS partners with the pseudo-orbital angular momentum $\tilde{l} = 2$, $p_{3/2}$, and $f_{5/2}$, as a function of the potential depth C.
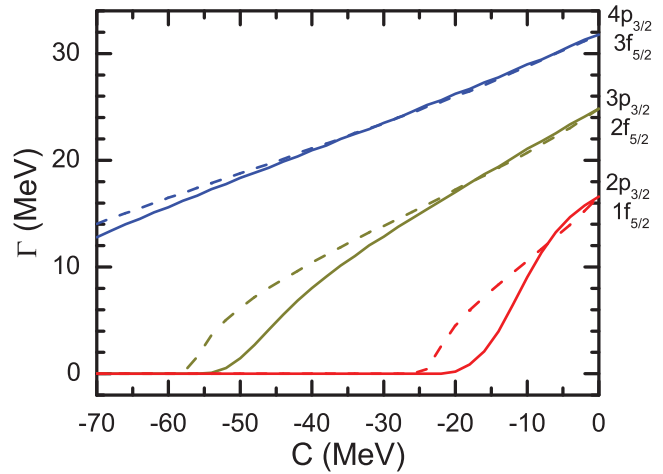

FIG. 8. (Color online) Widths of resonant states for $p_{3/2}$ and $f_{5/2}$ with $\tilde{l} = 2$ in spherical-well potentials as functions of the potential depth C. The results with pseudospin $\tilde{s} = \pm 1/2$ are denoted as solid and dashed curves, respectively.

There have been some investigations concerning the dependence of the PSS in resonant states on parameters, e.g., the depth, the radius, and the diffuseness, of Woods-Saxon potentials [89]. Differing from those studies, now by examining the Jost function, we are able to trace the PS partners from the case of finite potential depth to the PSS limit continuously. From this point of view, it is more helpful in understanding the origin and splitting of the PSS.

The energy splitting between PS partners with the pseudo-orbital angular momentum $\tilde{l} = 2$ ($p_{3/2}$ and $f_{5/2}$), is shown as a function of the potential depth C in Fig. 7. For simplicity, only results for the lowest three pairs are shown here. First, let us focus on the splitting of the lowest PS pair, the levels $2p_{3/2}$ and $1f_{5/2}$. When the potential depth increases from 0, the energy splitting first increases and then decreases until they encounter the threshold at a critical value of C, where one of the levels becomes a bound state and the splitting takes a minimum value. When the potential becomes even deeper, the splitting increases again. This kind of threshold effect is also observed for other PS pairs except that the critical value of C differs. The origin of this threshold effect should be one of the future topics concerning the PSS in resonant states.

In Fig. 8 we show the calculated widths of resonant states with $\tilde{l} = 2$ in square-well potentials as functions of the potential depth C. In this figure a zero width means the corresponding state has become a bound state. Similarly to the case of energies, the widths are also paired off when $C = 0$. Starting from the PSS limit, the width is a monotonically decreasing function of the potential depth. When the potential depth is finite, widths of a pair of pseudospin doublets differ. First, the level with $\tilde{s} = 1/2$ is wider. But at a critical value of C, there occurs a crossing between the two curves at which the two widths are the same. When the potential depth becomes even larger, the level with $\tilde{s} = -1/2$ becomes wider and the difference between two widths increases until it reaches a maximum value. Afterwards, the width splitting decreases until it becomes zero when both states become bound. This

anomalous variation tendency can be seen more clearly in Fig. 9 in which the width difference between PS partners, $\Delta\Gamma \equiv \Gamma_{\tilde{s}=-1/2} - \Gamma_{\tilde{s}=+1/2}$, is presented. The width splitting first decreases from zero to a maximum value with a negative sign and then increases and becomes zero. After the inversion of the width splitting, the splitting increases and reaches a maximum value and then becomes smaller again. For each PS pair, the width splitting assumes its largest value at some point above the corresponding threshold.

To now, we have examined the dependence of the PSS on the depth of the single-particle potential. From Eq. (16) one can also learn the dependence of the PSS on the radius of the potential R: With R increasing, the splitting term becomes smaller and the PSS is more conserved. There is no diffuseness in a square-well potential. It would be more useful to get
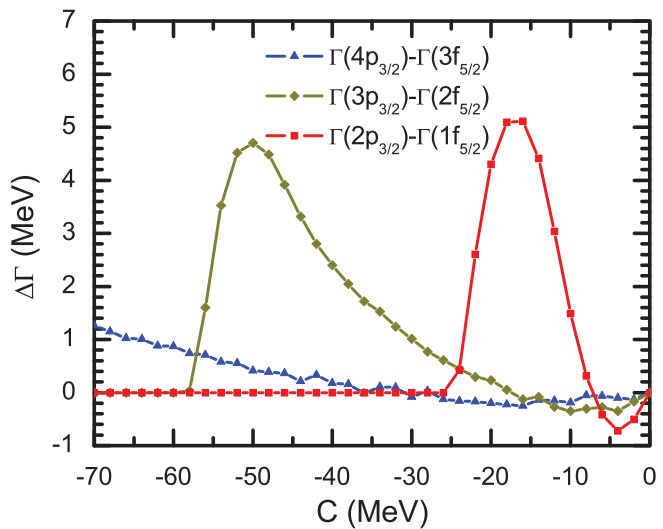

FIG. 9. (Color online) The width splitting between the PS partners with the pseudo-orbital angular momentum $\tilde{l} = 2$ ($p_{3/2}$ and $f_{5/2}$) as a function of the potential depth C.

analytic results for more realistic potentials. One then can discuss the PSS in single-particle resonant states in more realistic potentials.

IV. SUMMARY AND PERSPECTIVES

The pseudospin symmetry in single-particle resonant states is analyzed in detail in spherical square-well potentials. We built the Jost function for the small component of the Dirac wave function and studied resonant states as well as bound states by examining the zeros of the Jost function. The exact conservation and breaking of the PSS are investigated and a novel way is used to show the origin of the appearance of intruder states: The lowest zero of the Jost function with $\tilde{s} = -1/2$ is always isolated while the others are paired off with those of the Jost function with $\tilde{s} = +1/2$. When parameters of square-well potentials are fixed, we studied the dependence of the PSS on the energy and $\tilde{l}$ of pseudospin doublet states. It is found that the energy splitting is larger for higher pseudo-orbit angular momentum and at very high energies the splittings between PS partners are negligible. By examining the Jost function, we are able to trace continuously the PS partners from the PSS limit to the case with a finite potential depth. As the depth of the single-particle potential becomes deeper, the exact PSS begins to be broken and a threshold effect in the energy splitting is found: The energy splitting first increases and then decreases until the pseudospin doublets encounter the threshold where one of the levels becomes a bound state and the splitting takes a minimum value. When the potential becomes even deeper, the splitting increases again. When the depth of the single-particle potential increases from zero, an anomaly appears in the width splitting of PS partners: It, first, decreases from zero to a maximum value with a negative sign and then increases and becomes zero again; after the inversion of the width splitting, the splitting increases and reaches a maximum and positive value and then it becomes smaller and finally reaches zero.

Finally, we mention that the work presented in Ref. [92] and here extends the study of relativistic symmetries to resonant states. Although we have addressed several issues concerning the exact conservation and breaking mechanism of the PSS in single-particle resonant states, there are still many open problems [93], and we list several of them as follows:

  (i) Are there any experimental evidences of the PSS or SS in single-particle resonant states?

 (ii) Having in mind that the centrifugal barriers differ markedly for pseudospin doublets of single-particle resonant states, how to understand intuitively that their widths are exactly the same in the PSS limit?

(iii) Is the threshold effect found in the energy splitting of PS partners in spherical square-well potentials general for other potentials? If yes, what is its origin?

(iv) Is the anomaly found in the width splitting of PS partners in spherical square-well potentials general for other potentials? If yes, what is its origin?

 (v) What about the relations between Jost functions of pseudospin partners?

(vi) How about the PSS or SS in resonant states in antinucleon or antihyperon spectra?

(vii) How about the PSS or SS in resonant states in deformed systems?

(viii) What is the effect of the Coulomb interaction (e.g., for protons) on the PSS or SS symmetries?

[1] A. Arima, M. Harvey, and K. Shimizu, Phys. Lett. B **30**, 517 (1969).

[2] K. T. Hecht and A. Adler, Nucl. Phys. A **137**, 129 (1969).

[3] R. Ratna Raju, J. Draayer, and K. Hecht, Nucl. Phys. A **202**, 433 (1973).

[4] D. Troltenier, J. Draayer, P. Hess, and O. Castanos, Nucl. Phys. A **576**, 351 (1994); D. Troltenier, C. Bahri, and J. P. Draayer, *ibid.* **586**, 53 (1995).

[5] J. Dudek, W. Nazarewicz, Z. Szymanski, and G. A. Leander, Phys. Rev. Lett. **59**, 1405 (1987).

[6] C. Bahri, J. P. Draayer, and S. A. Moszkowski, Phys. Rev. Lett. **68**, 2133 (1992).

[7] W. Nazarewicz, M. A. Riley, and J. D. Garrett, Nucl. Phys. A **512**, 61 (1990).

[8] J. Y. Zeng, J. Meng, C. S. Wu, E. G. Zhao, Z. Xing, and X. Q. Chen, Phys. Rev. C **44**, R1745 (1991).

[9] Q. Xu, S. J. Zhu, J. H. Hamilton, A. V. Ramayya, J. K. Hwang, B. Qi, J. Meng, J. Peng, Y. X. Luo, J. O. Rasmussen, I. Y. Lee, S. H. Liu, K. Li, J. G. Wang, H. B. Ding, L. Gu, E. Y. Yeoh, and W. C. Ma, Phys. Rev. C **78**, 064301 (2008).

[10] W. Hua, X. H. Zhou, Y. H. Zhang, Y. Zheng, M. L. Liu, F. Ma, S. Guo, L. Ma, S. T. Wang, N. T. Zhang, Y. D. Fang, X. G. Lei, Y. X. Guo, M. Oshima, Y. Toh, M. Koizumi, Y. Hatsukawa, B. Qi, S. Q. Zhang, J. Meng, and M. Sugawara, Phys. Rev. C **80**, 034303 (2009).

[11] D. Troltenier, W. Nazarewicz, Z. Szymanski, and J. P. Draayer, Nucl. Phys. A **567**, 591 (1994).

[12] J. N. Ginocchio, Phys. Rev. C **59**, 2487 (1999); P. von Neumann-Cosel and J. N. Ginocchio, *ibid.* **62**, 014308 (2000).

[13] R. V. Jolos, N. Y. Shirikova, and A. V. Sushkov, Phys. Rev. C **86**, 044320 (2012).

[14] A. Bohr, I. Hamamoto, and B. R. Mottelson, Phys. Scr. **26**, 267 (1982).

[15] O. Castanos, M. Moshinsky, and C. Quesne, Phys. Lett. B **277**, 238 (1992).

[16] A. L. Blokhin, C. Bahri, and J. P. Draayer, Phys. Rev. Lett. **74**, 4149 (1995); J. Phys. A: Math. Gen. **29**, 2039 (1996); A. Blokhin, T. Beuschel, J. Draayer, and C. Bahri, Nucl. Phys. A **612**, 163 (1997); T. Beuschel, A. Blokhin, and J. Draayer, *ibid.* **619**, 119 (1997).

[17] J. N. Ginocchio, Phys. Rev. Lett. **78**, 436 (1997).

[18] J. Meng, K. Sugawara-Tanabe, S. Yamaji, P. Ring, and A. Arima, Phys. Rev. C **58**, R628 (1998).

[19] J. Meng, K. Sugawara-Tanabe, S. Yamaji, and A. Arima, Phys. Rev. C **59**, 154 (1999).

[20] A. Arima, "Dynamical symmetries and nuclear structure", RIKEN Preprint: RIKEN-AF-NP-276 (1999).

[21] P. Alberto, M. Fiolhais, M. Malheiro, A. Delfino, and M. Chiapparini, Phys. Rev. Lett. **86**, 5015 (2001).

[22] G. A. Lalazissis, Y. K. Gambhir, J. P. Maharana, C. S. Warke, and P. Ring, Phys. Rev. C **58**, R45 (1998).

[23] K. Sugawara-Tanabe and A. Arima, Phys. Rev. C **58**, R3065 (1998); **60**, 019901(E) (1999).

[24] J. N. Ginocchio and D. G. Madland, Phys. Rev. C **57**, 1167 (1998); J. N. Ginocchio, *ibid.* **66**, 064312 (2002).

[25] K. Sugawara-Tanabe, S. Yamaji, and A. Arima, Phys. Rev. C **65**, 054313 (2002).

[26] J. N. Ginocchio, A. Leviatan, J. Meng, and S.-G. Zhou, Phys. Rev. C **69**, 034303 (2004).

[27] S.-G. Zhou, J. Meng, and P. Ring, Phys. Rev. C **68**, 034323 (2003); AIP Conf. Proc. **865**, 90 (2006); in *Physics of Unstable Nuclei*, edited by D. T. Khoa, P. Egelhof, S. Gales, N. Van Giai, and T. Motobayashi (World Scientific, Singapore, 2008), pp. 402–408.

[28] S.-G. Zhou, J. Meng, P. Ring, and E.-G. Zhao, Phys. Rev. C **82**, 011301(R) (2010); L. Li, J. Meng, P. Ring, E.-G. Zhao, and S.-G. Zhou, *ibid.* **85**, 024312 (2012); Chin. Phys. Lett. **29**, 042101 (2012); AIP Conf. Proc. **1491**, 208 (2012); **1529**, 190 (2013).

[29] Y. Chen, L. Li, H. Liang, and J. Meng, Phys. Rev. C **85**, 067301 (2012).

[30] N. Schunck and J. L. Egido, Phys. Rev. C **77**, 011301(R) (2008); **78**, 064305 (2008).

[31] W. H. Long, P. Ring, N. Van Giai, and J. Meng, Phys. Rev. C **81**, 024308 (2010).

[32] J. N. Ginocchio, Phys. Rep. **315**, 231 (1999).

[33] S.-G. Zhou, J. Meng, and P. Ring, Phys. Rev. Lett. **91**, 262501 (2003).

[34] X. T. He, S. G. Zhou, J. Meng, E. G. Zhao, and W. Scheid, Eur. Phys. J. A **28**, 265 (2006).

[35] H. Liang, W. Hui Long, J. Meng, and N. Van Giai, Eur. Phys. J. A **44**, 119 (2010).

[36] I. N. Mishustin, L. M. Satarov, T. J. Burvenich, H. Stocker, and W. Greiner, Phys. Rev. C **71**, 035201 (2005).

[37] C.-Y. Song, J.-M. Yao, and J. Meng, Chin. Phys. Lett. **26**, 122102 (2009); **28**, 092101 (2011); C.-Y. Song and J.-M. Yao, Chin. Phys. C **34**, 1425 (2010).

[38] J. N. Ginocchio, Phys. Rep. **414**, 165 (2005).

[39] H. Liang, S. Shen, P. Zhao, and J. Meng, Phys. Rev. C **87**, 014334 (2013); S. Shen, H. Liang, P. Zhao, S. Zhang, and J. Meng, *ibid.* **88**, 024311 (2013).

[40] A. Leviatan and J. N. Ginocchio, Phys. Lett. B **518**, 214 (2001).

[41] S. Marcos, M. Lopez-Quelle, R. Niembro, and L. N. Savushkin, Eur. Phys. J. A **34**, 429 (2007); **37**, 251 (2008); J. Phys: Conf. Ser. **128**, 012034 (2008); B. Desplanques and S. Marcos, Eur. Phys. J. A **43**, 369 (2010).

[42] C. Jia, P. Guo, Y. Diao, L. Yi, and X. Xie, Eur. Phys. J. A **34**, 41 (2007).

[43] F.-L. Zhang, B. Fu, and J.-L. Chen, Phys. Rev. A **78**, 040101 (2008); **80**, 054102 (2009); F.-L. Zhang and J.-L. Chen, J. Math. Phys. **50**, 032301 (2009).

[44] M.-C. Zhang, G.-Q. Huang-Fu, and B. An, Phys. Scr. **80**, 065018 (2009); M.-C. Zhang, Cent. Eur. J. Phys. **7**, 768 (2009); Int. J. Theor. Phys. **48**, 2625 (2009); M.-C. Zhang and G.-Q. Huang-Fu, J. Math. Phys. **52**, 053518 (2011).

[45] M. R. Setare and Z. Nazari, Acta Phys. Pol. B **40**, 2809 (2009); **41**, 2459 (2010); Mod. Phys. Lett. A **25**, 549 (2010).

[46] G.-F. Wei and S.-H. Dong, Phys. Lett. B **686**, 288 (2010); Eur. Phys. J. A **43**, 185 (2010); W.-L. Chen and G.-F. Wei, Chin. Phys. B **20**, 062101 (2011).

[47] O. Aydogdu and R. Sever, Eur. Phys. J. A **43**, 73 (2010); Phys. Lett. B **703**, 379 (2011); O. Aydogdu, E. Maghsoodi, and H. Hassan, Chin. Phys. B **22**, 010302 (2013).

[48] H. Akcay, Phys. Lett. A **373**, 616 (2009); H. Akcay and C. Tezcan, Int. J. Mod. Phys. C **20**, 930 (2009).

[49] M. Hamzavi, A. A. Rajabi, and H. Hassanabadi, Phys. Lett. A **374**, 4303 (2010); S. Ikhdair and M. Hamzavi, Few-Body Syst. **53**, 473 (2012); M. Hamzavi, S. M. Ikhdair, and K.-E. Thylwe, Int. J. Mod. Phys. E **21**, 1250097 (2012); M. Hamzavi and A. A. Rajabi, Adv. High Ener. Phys. **2013**, 196986 (2013).

[50] S. Zarrinkamar, H. Hassanabadi, and A. A. Rajabi, Int. J. Mod. Phys. A **26**, 1011 (2011); H. Hassanabadi, E. Maghsoodi, S. Zarrinkamar, and H. Rahimov, Chin. Phys. B **21**, 120302 (2012); E. Maghsoodi, H. Hassanabadi, S. Zarrinkamar, and H. Rahimov, Phys. Scr. **85**, 055007 (2012).

[51] N. Candemir, Int. J. Mod. Phys. E **21**, 1250060 (2012).

[52] Y. Z. Wang, G. L. Yu, Z. Y. Li, and J. Z. Gu, J. Phys. G: Nucl. Part. Phys. **40**, 045105 (2013).

[53] B. J. Falaye and S. M. Ikhdair, Chin. Phys. B **22**, 060305 (2013).

[54] R. Lisboa, M. Malheiro, A. S. de Castro, P. Alberto, and M. Fiolhais, Phys. Rev. C **69**, 024319 (2004); P. Alberto, R. Lisboa, M. Malheiro, and A. S. de Castro, *ibid.* **71**, 034313 (2005); A. S. de Castro, P. Alberto, R. Lisboa, and M. Malheiro, *ibid.* **73**, 054309 (2006); L. B. Castro, *ibid.* **86**, 052201 (2012).

[55] W. H. Long, H. Sagawa, N. V. Giai, and J. Meng, Phys. Rev. C **76**, 034314 (2007).

[56] W. H. Long, P. Ring, J. Meng, N. Van Giai, and C. A. Bertulani, Phys. Rev. C **81**, 031302(R) (2010).

[57] S. Typel, Nucl. Phys. A **806**, 156 (2008).

[58] R. Lisboa, M. Malheiro, P. Alberto, M. Fiolhais, and A. S. de Castro, Phys. Rev. C **81**, 064324 (2010); A. S. de Castro and P. Alberto, Phys. Rev. A **86**, 032122 (2012).

[59] H. Liang, P. Zhao, Y. Zhang, J. Meng, and N. V. Giai, Phys. Rev. C **83**, 041301(R) (2011); F.-Q. Li, P.-W. Zhao, and H.-Z. Liang, Chin. Phys. C **35**, 825 (2011).

[60] A. Leviatan, Phys. Rev. Lett. **103**, 042502 (2009).

[61] J.-Y. Guo, Phys. Rev. C **85**, 021302(R) (2012); D.-P. Li, S.-W. Chen, and J.-Y. Guo, *ibid.* **87**, 044311 (2013).

[62] R. Jolos and V. Voronov, Phys. At. Nucl. **70**, 812 (2007).

[63] J. J. Li, W. H. Long, J. Margueron, and N. Van Giai, arXiv:1303.2765 [nucl-th] (2013).

[64] P. Alberto, A. S. de Castro, and M. Malheiro, Phys. Rev. C **87**, 031301(R) (2013).

[65] T.-S. Chen, H.-F. Lü, J. Meng, S.-Q. Zhang, and S.-G. Zhou, Chin. Phys. Lett. **20**, 358 (2003); T.-S. Chen, H.-F. Lu, J. Meng, and S.-G. Zhou, High Ener. Phys. Nucl. Phys. **27**, 324 (2003), in Chinese.

[66] R. Furnstahl and B. D. Serot, Nucl. Phys. A **673**, 298 (2000).

[67] H.-W. Ke, Z. Li, J.-L. Chen, Y.-B. Ding, and X.-Q. Li, Int. J. Mod. Phys. A **25**, 1123 (2010).

[68] J. Dobaczewski, H. Flocard, and J. Treiner, Nucl. Phys. A **422**, 103 (1984); J. Dobaczewski, W. Nazarewicz, T. R. Werner, J. F. Berger, C. R. Chinn, and J. Dechargé, Phys. Rev. C **53**, 2809 (1996).

[69] J. Meng and P. Ring, Phys. Rev. Lett. **77**, 3963 (1996); **80**, 460 (1998); J. Meng, Nucl. Phys. A **635**, 3 (1998); J. Meng, H. Toki, J. Y. Zeng, S. Q. Zhang, and S.-G. Zhou, Phys. Rev. C **65**, 041302(R) (2002); J. Meng, H. Toki, S. G. Zhou, S. Q. Zhang, W. H. Long, and L. S. Geng, Prog. Part. Nucl. Phys. **57**, 470 (2006); J. Meng, Z. Niu, H. Liang, and B. Sun, Sci. China-Phys. Mech. Astron. **54**(Suppl. 1), 119 (2011).

[70] W. Pöschl, D. Vretenar, G. A. Lalazissis, and P. Ring, Phys. Rev. Lett. **79**, 3841 (1997); D. Vretenar, A. Afanasjev, G. Lalazissis, and P. Ring, Phys. Rep. **409**, 101 (2005).

[71] Y. Zhang, M. Matsuo, and J. Meng, Phys. Rev. C **83**, 054301 (2011); **86**, 054318 (2012).

[72] J. C. Pei, M. V. Stoitsov, G. I. Fann, W. Nazarewicz, N. Schunck, and F. R. Xu, Phys. Rev. C **78**, 064306 (2008); J. C. Pei, A. T. Kruppa, and W. Nazarewicz, *ibid.* **84**, 024311 (2011); J. C. Pei, Y. N. Zhang, and F. R. Xu, *ibid.* **87**, 051302(R) (2013).

[73] J. He, J. Hu, S. Xu, Z. Chen, X. Zhang, J. Wang, X. Yu, L. Zhang, L. Li, Y. Yang, P. Ma, X. Zhang, Z. Hu, Z. Guo, X. Xu, X. Yuan, W. Lu, Y. Yu, Y. Zang, S. Tang, R. Ye, J. Chen, S. Jin, C. Du, S. Wang, J. Ma, L. Liu, Z. Bai, X. Lei, Z. Sun, Y. Zhang, X. Zhou, H. Xu, J. Su, E. Li, H. Wang, W. Tian, and X. Li, Sci. China-Phys. Mech. Astron. **54**(Suppl. 1), 32 (2011).

[74] C. Lin, X. Xu, H. Jia, F. Yang, F. Jia, Z. Wu, S. Zhang, Z. Liu, H. Zhang, H. Xu, Z. Sun, J. Wang, Z. Hu, M. Wang, R. Chen, X. Zhang, C. Li, X. Lei, Z. Xu, G. Xiao, and W. Zhan, Sci. China-Phys. Mech. Astron. **54**(Suppl. 1), 73 (2011).

[75] L. Lü, Y. Ye, D. Jiang, H. Hua, T. Zheng, Z. Li, Y. Ge, X. Li, J. Lou, Z. Cao, Y. Song, J. Xiao, Q. Li, R. Qiao, H. You, R. Chen, H. Xu, J. Wang, Z. Guo, X. Zhang, C. Li, Z. Hu, R. Chen, M. Wang, Z. Xu, K. Yue, B. Tang, Y. Zang, X. Zhang, X. Yao, J. Chen, and Z. Bai, Sci. China-Phys. Mech. Astron. **54**(Suppl. 1), 136 (2011).

[76] V. I. Kukulin, V. M. Krasnopol'sky, and J. Horácek, *Theory of Resonances: Principles and Applications* (Kluwer Academic, Dordrecht, 1989).

[77] S.-C. Yang, J. Meng, and S.-G. Zhou, Chin. Phys. Lett. **18**, 196 (2001).

[78] S. S. Zhang, J. Meng, S. G. Zhou, and G. C. Hillhouse, Phys. Rev. C **70**, 034308 (2004); S. S. Zhang, W. Zhang, S. G. Zhou, and J. Meng, Eur. Phys. J. A **32**, 43 (2007); S. S. Zhang, Int. J. Mod. Phys. E **18**, 1761 (2009); S.-S. Zhang, M. S. Smith, G. Arbanas, and R. L. Kozub, Phys. Rev. C **86**, 032802 (2012); S.-S. Zhang, X.-D. Xu, and J.-P. Peng, Eur. Phys. J. A **48**, 40 (2012).

[79] L. Zhang, S.-G. Zhou, J. Meng, and E.-G. Zhao, Phys. Rev. C **77**, 014312 (2008); Acta Phys. Sinica **56**, 3839 (2007), in Chinese; S.-G. Zhou, J. Meng, and E.-G. Zhao, J. Phys. B: At. Mol. Phys. **42**, 245001 (2009).

[80] H. Mei, J. M. Yao, and H. Chen, Chin. Phys. C **33**, 113 (2009).

[81] Z.-Z. Zhang, Chin. Phys. C **33**, 187 (2009); Z.-Z. Zhang, H. Lin, and Y.-M. Mi, Mod. Phys. Lett. A **25**, 727 (2010).

[82] J.-Y. Guo, X.-Z. Fang, P. Jiao, J. Wang, and B.-M. Yao, Phys. Rev. C **82**, 034318 (2010); J.-Y. Guo, J. Wang, B.-M. Yao, and P. Jiao, Int. J. Mod. Phys. E **19**, 1357 (2010); J.-Y. Guo, M. Yu, J. Wang, B.-M. Yao, and P. Jiao, Comput. Phys. Commun. **181**, 550 (2010); Q. Liu, J.-Y. Guo, Z.-M. Niu, and S.-W. Chen, Phys. Rev. C **86**, 054312 (2012).

[83] K. Hagino and N. Van Giai, Nucl. Phys. A **735**, 55 (2004).

[84] Z. P. Li, J. Meng, Y. Zhang, S. G. Zhou, and L. N. Savushkin, Phys. Rev. C **81**, 034311 (2010); Z.-P. Li, Y. Zhang, D. Vretenar, and J. Meng, Sci. China Phys. Mech. Astron. **53**, 773 (2010).

[85] D. Fedorov, A. Jensen, M. Thogersen, E. Garrido, and R. de Diego, Few-Body Syst. **45**, 191 (2009).

[86] F. M. Fernandez, Appl. Math. Comput. **218**, 5961 (2012).

[87] J. N. Ginocchio, Phys. Rev. Lett. **82**, 4599 (1999); Phys. Rev. C **65**, 054002 (2002).

[88] H. Leeb and S. Wilmsen, Phys. Rev. C **62**, 024602 (2000); H. Leeb and S. A. Sofianos, *ibid.* **69**, 054608 (2004).

[89] J.-Y. Guo, R.-D. Wang, and X.-Z. Fang, Phys. Rev. C **72**, 054319 (2005); J. Y. Guo and X. Z. Fang, *ibid.* **74**, 024320 (2006); Q. Liu, Z.-M. Niu, and J.-Y. Guo, Phys. Rev. A **87**, 052122 (2013).

[90] S.-S. Zhang, W. Zhang, B.-H. Sun, J.-Y. Guo, and S.-G. Zhou, High Ener. Phys. Nucl. Phys. **30**(S2), 97 (2006); S.-S. Zhang, B.-H. Sun, and S.-G. Zhou, Chin. Phys. Lett. **24**, 1199 (2007).

[91] Q. Xu and J.-Y. Guo, Int. J. Mod. Phys. E **21**, 1250096 (2012).

[92] B.-N. Lu, E.-G. Zhao, and S.-G. Zhou, Phys. Rev. Lett. **109**, 072501 (2012).

[93] B.-N. Lu, E.-G. Zhao, and S.-G. Zhou, AIP Conf. Proc. **1533**, 63 (2013).

[94] B. D. Serot and J. D. Walecka, Adv. Nucl. Phys. **16**, 1 (1986).

[95] P. G. Reinhard, Rep. Prog. Phys. **52**, 439 (1989).

[96] P. Ring, Prog. Part. Nucl. Phys. **37**, 193 (1996); **46**, 165 (2001).

[97] N. Paar, D. Vretenar, and G. Colo, Rep. Prog. Phys. **70**, 691 (2007).

[98] J. Meng, J. Peng, S.-Q. Zhang, and P.-W. Zhao, Front. Phys. **8**, 55 (2013).

[99] Y. Zhang, H.-Z. Liang, and J. Meng, Int. J. Mod. Phys. E **19**, 55 (2010); Chin. Phys. C **33**(Suppl. I), 113 (2009); Chin. Phys. Lett. **26**, 092401 (2009); F.-Q. Li, Y. Zhang, H.-Z. Liang, and J. Meng, Sci. China-Phys. Mech. Astron. **54**, 231 (2011).

[100] P. W. Zhao, Z. P. Li, J. M. Yao, and J. Meng, Phys. Rev. C **82**, 054319 (2010); P. W. Zhao, J. Peng, H. Z. Liang, P. Ring, and J. Meng, Phys. Rev. Lett. **107**, 122501 (2011).

[101] A. Leviatan, Phys. Rev. Lett. **92**, 202501 (2004).

[102] P. Alberto, M. Fiolhais, M. Malheiro, A. Delfino, and M. Chiapparini, Phys. Rev. C **65**, 034307 (2002).